JACC: BASIC TO TRANSLATIONAL SCIENCE
PUBLISHED BY ELSEVIER ON BEHALF OF THE AMERICAN COLLEGE OF CARDIOLOGY FOUNDATION.

VOL. 5, NO. 2, 2020

CLINICAL RESEARCH

Reduced Left Atrial Emptying Fraction and Chymase Activation in Pathophysiology of Primary Mitral Regurgitation

Brittany Butts, PhD,[a] Mustafa I. Ahmed, MD,[a] Navkaranbir S. Bajaj, MD, MPH,[a] Pamela Cox Powell, MS,[a] Betty Pat, PhD,[a] Silvio Litovsky, MD,[b] Himanshu Gupta, MD,[a,c,d] Steven G. Lloyd, MD,[a,c] Thomas S. Denney, PhD,[e] Xiaoxia Zhang, PhD,[e] Inmaculada Aban, PhD,[f] Sakthivel Sadayappan, PhD, MBA,[g] James W. McNamara, PhD,[g] Michael J. Watson, PhD,[h] Carlos M. Ferrario, MD,[i] James F. Collawn, PhD,[j] Clifton Lewis, MD,[k] James E. Davies, MD,[k] Louis J. Dell'Italia, MD[a,c]

VISUAL ABSTRACT

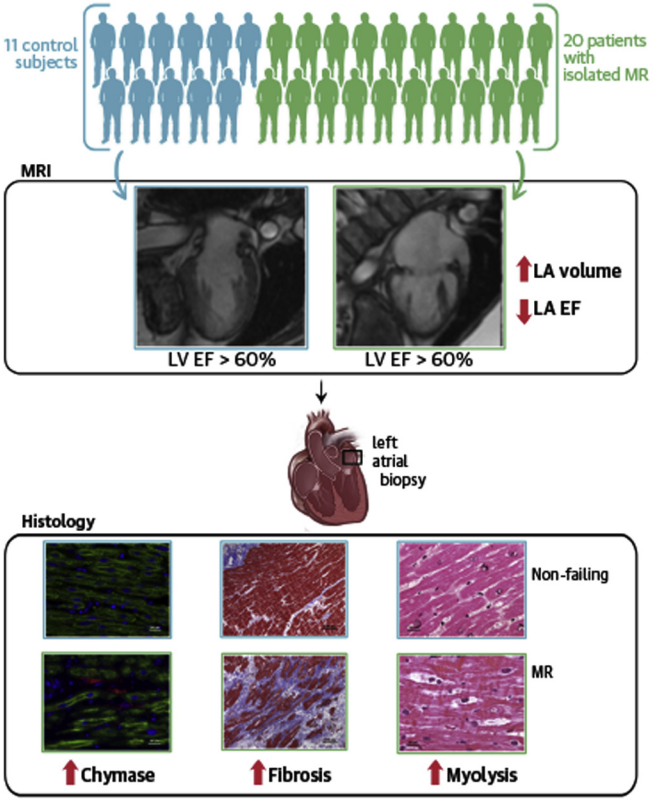

Butts, B. et al. J Am Coll Cardiol Basic Trans Science. 2020;5(2):109–22.

ISSN 2452-302X https://doi.org/10.1016/j.jacbts.2019.11.006

ABBREVIATIONS AND ACRONYMS

EF = ejection fraction

LA = left atrial

LA EF = left atrial emptying fraction

LV = left ventricle

MR = mitral regurgitation

MV = mitral valve

RA = right atrial

TEM = transmission electron microscopy

TGF = transforming growth factor

HIGHLIGHTS

- **Extensive LA fibrosis is related to an increase in LA size and decrease in total LA EF. This supports the contention that the LA is not merely a bystander of MR but rather is actively involved in the pathophysiology of MR.**
- **Chymase is plentiful in the human heart, especially in the LA, and correlates with extracellular matrix accumulation in primary MR.**
- **Because of the unreliability of the LV ejection fraction in primary MR, future studies may consider LA size and total LA EF for timing of surgical intervention of asymptomatic moderate to severe MR.**

SUMMARY

Increasing left atrial (LA) size predicts outcomes in patients with isolated mitral regurgitation (MR). Chymase is plentiful in the human heart and affects extracellular matrix remodeling. Chymase activation correlates to LA fibrosis, LA enlargement, and a decreased total LA emptying fraction in addition to having a potential intracellular role in mediating myofibrillar breakdown in LA myocytes. Because of the unreliability of the left ventricular ejection fraction in predicting outcomes in MR, LA size and the total LA emptying fraction may be more suitable indicators for timing of surgical intervention. (J Am Coll Cardiol Basic Trans Science 2020;5:109–22) Published by Elsevier on behalf of the American College of Cardiology Foundation.

There is an unexpected decrease in left ventricular (LV) ejection fraction of <50% in 20% of patients with primary degenerative mitral regurgitation (MR) after mitral valve (MV) surgery, despite having a presurgical LV ejection fraction of 65% and LV end-systolic dimension <4.0 cm (1–3). Left atrial (LA) size is associated with a poor prognosis, despite LV ejection fractions of >60% (4,5). A number of studies have identified extensive LA myolysis, mitochondrial damage, and interstitial fibrosis in patients with degenerative MR (6–9). However, these ultrastructural changes are not connected to LA volumes or to the LA total emptying fraction (LA EF). Total LA EF and LA minimum volume have been shown to correlate with LV end-diastolic pressure obtained at cardiac catheterization (10).

SEE PAGE 123

We reported increased chymase activity in the LA of patients who underwent the MAZE procedure (Surgical procedure creating a pattern or “maze” of scar tissue in the atria to treat atrial fibrillation.) for atrial fibrillation (11). Chymase is an abundant protein in the human heart with highly efficient angiotensin II–forming activity (12). The proteolytic actions of chymase include activation of transforming growth

From the [a]Department of Medicine, Division of Cardiovascular Disease, University of Alabama at Birmingham, Birmingham, Alabama; [b]Department of Pathology, University of Alabama at Birmingham, Birmingham, Alabama; [c]Department of Veterans Affairs Medical Center, Birmingham, Alabama; [d]Department of Cardiology, Valley Health System, Paramus, New Jersey; [e]Department of Electrical and Computer Engineering, Auburn University School of Engineering, Auburn, Alabama; [f]Department of Biostatistics, University of Alabama at Birmingham, Birmingham, Alabama; [g]Division of Cardiovascular Disease, University of Cincinnati College of Medicine, Cincinnati, Ohio; [h]Division of Cardiothoracic Surgery, Department of Surgery, Duke University, Durham, North Carolina; [i]Department of Surgery, Wake Forest University Health Science Center, Winston-Salem, North Carolina; [j]Department of Cell, Developmental, and Integrative Biology, University of Alabama at Birmingham, Birmingham, Alabama; and the [k]Department of Surgery, Division of Thoracic and Cardiovascular Surgery, University of Alabama at Birmingham, Birmingham, Alabama. Drs. Ferrario and Dell’Italia were supported by the National Heart, Lung, and Blood Institute (NHLBI) (P01 HL051952). Dr. Dell’Italia was supported by the NHLBI and the Specialized Centers of Clinically Oriented Research (P50HL077100), by the National Institutes of Health National Center for Medical Rehabilitation Research (4T32HD071866), and by the Department of Veteran Affairs for Merit Review (1CX000993-01). Dr. Bajaj was supported by an American College of Cardiology Presidential Career Development award, Walter B. Frommeyer, Junior Fellowship in Investigative Medicine and National Center for Advancing Translational Research of the National Institutes of Health (UL1TR001417). Dr. Sadayappan is a consultant with Amgen, Merck, MyoKardia, Red Saree Inc., Leducq Foundation, and AstraZeneca. All other authors have reported that they have no relationships relevant to the contents of this paper to disclose.

The authors attest they are in compliance with human studies committees and animal welfare regulations of the authors’ institutions and Food and Drug Administration guidelines, including patient consent where appropriate. For more information, visit the *JACC: Basic to Translational Science* author instructions page.

Manuscript received October 1, 2019; revised manuscript received November 4, 2019, accepted November 4, 2019.

factor (TGF)-β and conversion of prepro endothelin 1 to endothelin 1, which results in increased extracellular matrix production (12). Chymase also degrades fibronectin, which leads to cell apoptosis and activates matrix metalloproteinases, multiple cytokines, and stem cell factor that mediates inflammatory cell infiltration (12). In addition to these extracellular actions, there is emerging evidence of chymase within cardiomyocytes, which raises the possibility of intracellular protease targets (13,14).

In the present investigation of patients with isolated MR, we demonstrated a marked increase in LA tissue chymotryptic-like activity and extensive fibrosis, as well as chymase within LA myocytes in association with intracellular chymotryptic activity and myosin breakdown. Furthermore, LA chymase activity was related to LA fibrosis and to the severity of LA dysfunction obtained by serial short-axis cardiac magnetic resonance imaging that covered the ventricles and atria for LA volume calculations that were independent of geometric assumptions.

METHODS

PATIENTS. The study protocol was approved by the University of Alabama at Birmingham Institutional Review Board, and informed consent was obtained from 20 patients with isolated MR secondary to degenerative MV disease (Supplemental Table 1) and 11 control subjects. Control subjects did not have a history of cardiovascular disease and smoking and were not taking any cardiovascular medication. Severe MR was documented on echocardiography and/or Doppler studies in all cases. Exclusion criteria were previous myocardial infarction, infectious or inflammatory disease, autoimmune disease, malignancy, chronic renal failure (serum creatinine >2.5 mg/dl), acute or chronic viral hepatitis, or use of immunosuppressive drugs. All patients had cardiac catheterization before surgery. Patients with obstructive coronary artery disease (>50% stenosis), aortic valve disease, or concomitant mitral stenosis were excluded. All patients had a degenerative MV, manifested by thickening and prolapse of the MV on echocardiography, and Carpentier II MV disease documented at surgery. Biopsy tissue was taken from the LA between the right superior and inferior pulmonary veins, a right atrial (RA) sample was taken from the RA appendage, and LV tissue was taken from the posterior endocardial wall.

NONFAILING HEART SAMPLES. Human samples of the RA, LA, and LV were obtained from the Duke Heart Repository under their approved Duke biorepository institutional review board protocol from donors confirmed brain dead and who had had a LV ejection fraction >50% (Supplemental Table 2). When procuring an organ for transplantation, donor specimens were removed and arrested from the donor and flushed with cold cardioplegic solution, which preserved the organ during transport. Tissue was collected from hospitals in North Carolina to minimize transport time to the Duke University Medical Center. Upon arrival, specimens were immediately sectioned and frozen in liquid nitrogen.

CARDIAC MAGNETIC RESONANCE IMAGING. Patients underwent cardiac magnetic resonance imaging within 1 month before MV surgery on a 1.5-T scanner (Signa, GE, Milwaukee, Wisconsin). Normal subjects and patients with MR were imaged with standard cardiac cine slices in the 2- and 4-chamber views, as well as a short-axis view that covered the whole ventricles and atria. Parameters were set as follows: field of view of 360 to 400 mm; 8-mm slice thickness; no gap; and 256 × 128 matrix. In short axis (SA) views, endocardial contours were manually drawn at ventricular end-diastole and end-systole continuously from the LV apex to LA apex and from the RV apex to RA apex. Intersections of the MV and tricuspid valve leaflets with the LV and RV walls were manually placed in left 2-chamber and 4-chamber views and a right 2-chamber view at end-diastole and end-systole. All intersections and endocardial contours were propagated to the remaining time frames using an automated algorithm (15,16). Planes were fit to the mitral and tricuspid annuli based on the MV and tricuspid valve intersections and used to determine which contour points were part of the LV and/or RV and which contour points were part of the LA and/or RA. Chamber volumes were computed in each time frame by summing the volumes in each slice defined by the endocardial contours. MR regurgitant fraction and regurgitant volume were derived from the difference between LV and RV stroke volumes. No patient had significant tricuspid regurgitation.

TRANSMISSION ELECTRON MICROSCOPY. Ten MR biopsies were fixed in 2.5% Glutaraldehyde/Sorensen's Phosphate Buffer (Electron Microscopy Sciences #15980, Hatfield, Pennsylvania) overnight at 4°C, as previously described by our laboratory (17,18). For details, see the Supplemental Appendix.

IMMUNOHISTOCHEMISTRY. MR and nonfailing heart specimens were immersion-fixed in 10% buffered formalin, paraffin-embedded, sectioned (4 to 5 μm), and processed for hematoxylin and eosin and immunohistochemistry. Sections (5 μm) were stained using desmin (Abcam #ab15200, 1:200, Cambridge, Massachusetts), chymase (Abcam #ab2377, 1:50), and

FIGURE 1 Box Plots and Time–Volume Curves

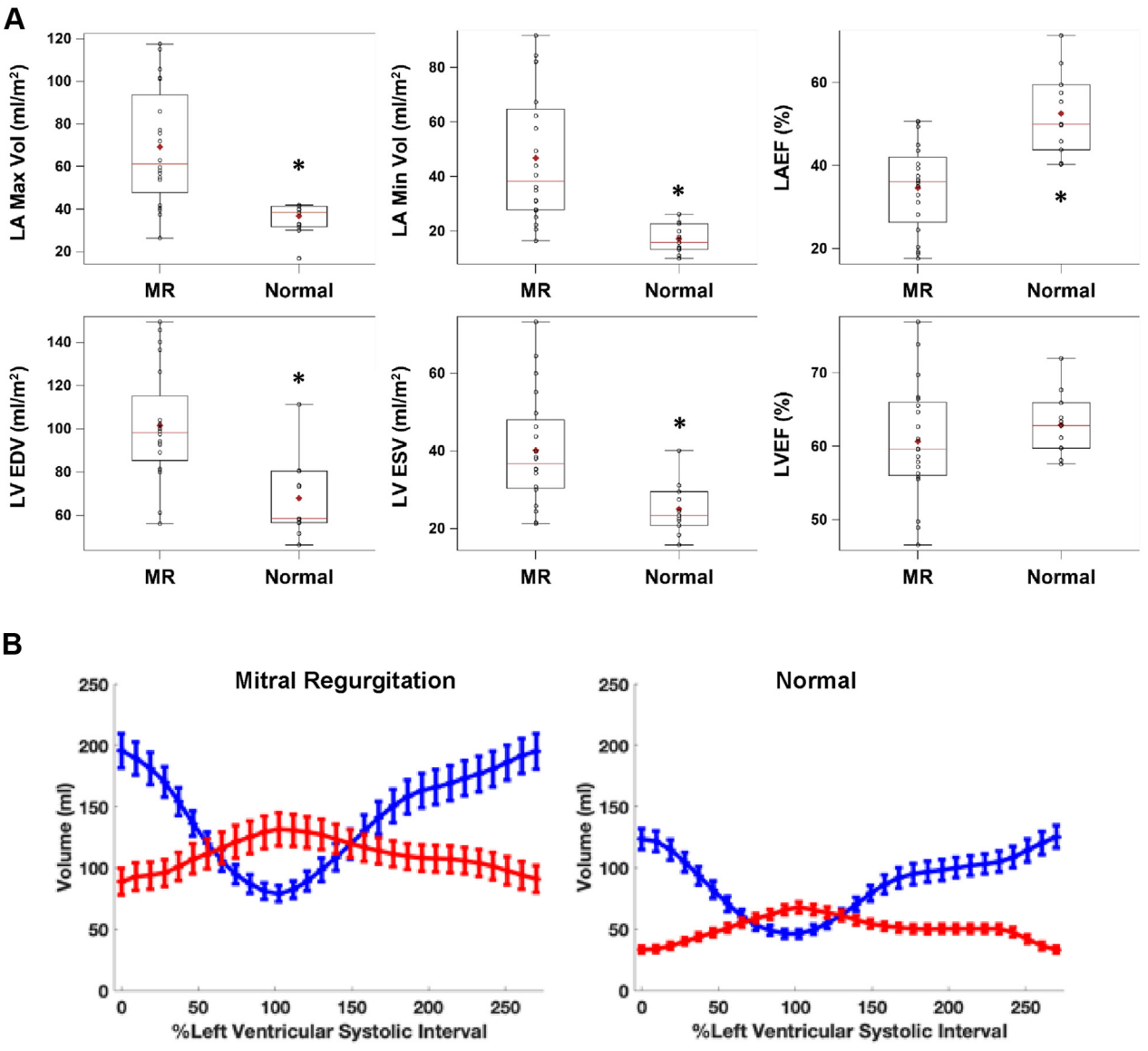

(A) Box plots demonstrating the significant increase in left atrial (LA) and left ventricular (LV) maximum and minimum volume and the decrease in the total LA emptying fraction (LA EF) in patients with mitral regurgitation (MR) (n = 20) versus normal subjects (n = 11). *p < 0.001. **(B)** LA **(red)** and LV **(blue)** time–volume curves for the 20 patients with (MR) and 11 normal subjects. LVEDV = left ventricular end-diastolic volume; LVEF = left ventricular ejection fraction; LVESV = left ventricular end-systolic volume.

Alexa Fluor 488- and 594-conjugated secondary antibodies (1:700, Life Technologies, Carlsbad, California) (17,18). Nuclei were labeled with 4,6-diamidino-2-phenylindole (DAPI) (1.5 μg/ml, Vector Laboratories #H-1500, Burlingame, California), as previously described by our laboratory (17,18).

TGF-β_1 MEASUREMENT. TGF-β_1 in LA tissue lysates was measured with the Quantikine ELISA Human TGFβ_1 kit (R&D Systems, Minneapolis, Minnesota). For details, see the Supplemental Appendix.

COLLAGEN ANALYSIS. Collagen quantification was performed on MR and nonfailing atrial, paraffin-embedded 4-μm sections stained with picric acid Sirius red F3BA. For details, see the Supplemental Appendix.

IN SITU CHYMOTRYPTIC ACTIVITY. Intracellular chymase activity was verified by in situ chymotryptic

FIGURE 2 Cardiac Magnetic Resonance and 3D Images

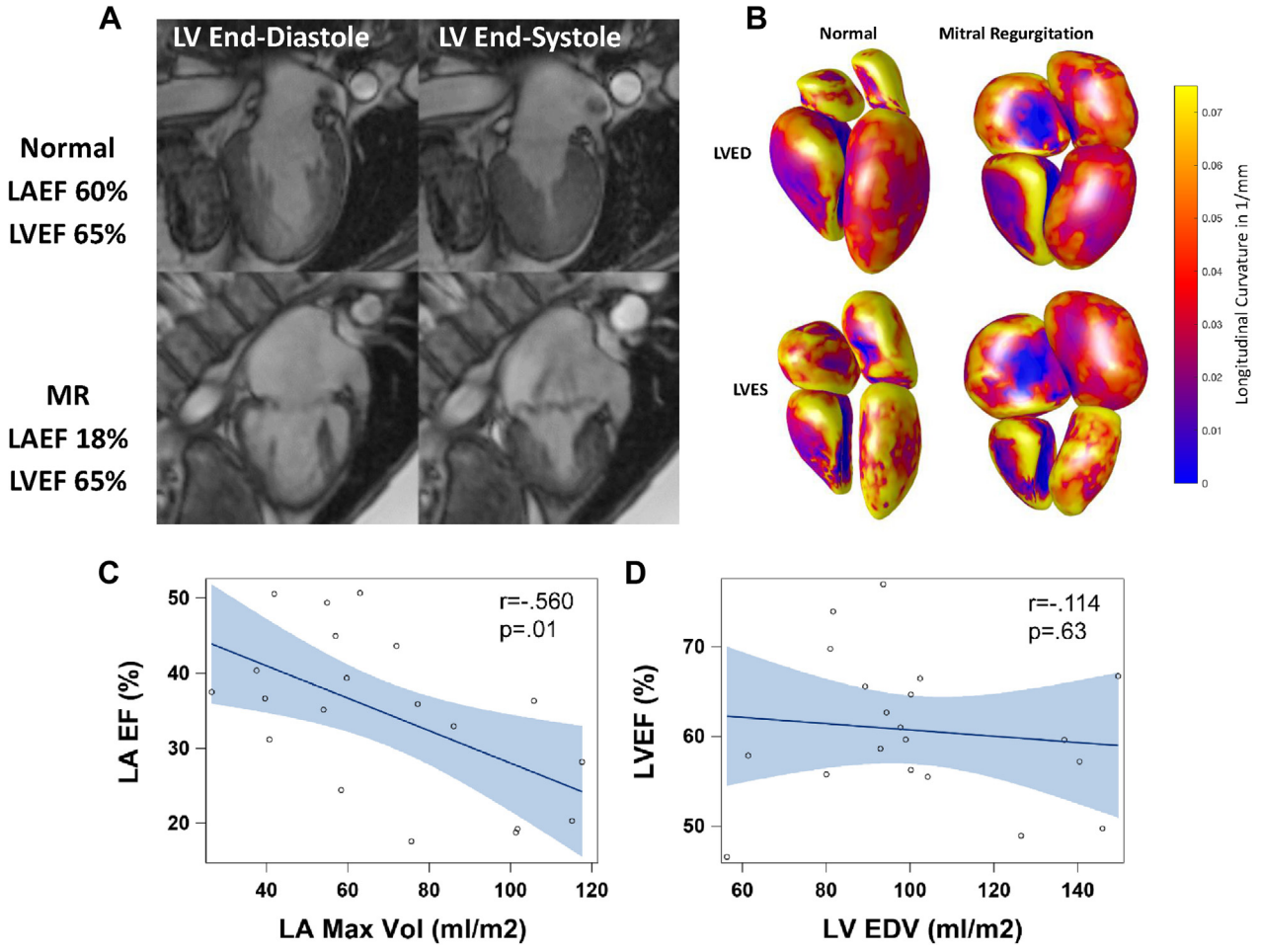

(A) Cardiac magnetic resonance images of a normal subject **(upper panels)** and patient with MR **(lower panels)** at LV end-diastole (LVED) and end-systole (LVES). MR LA is markedly enlarged at maximum **(right)** and minimum **(left)** volume with total LA EF of 18% and LVEF of >60%. **(B)** Three-dimensional images of color surface longitudinal curvature demonstrated the global decrease in curvature and marked dilatation in the patients with MR. **(C)** LA EF is negatively related to increasing LA maximum volume **(C)**, whereas **(D)** LVEF does not relate to LVEDV. Abbreviations as in Figure 1.

activity as described previously by our laboratory (13). For details, see the Supplemental Appendix.

CHYMASE mRNA PRODUCTION BY IN SITU HYBRIDIZATION. The expression of human chymase (CMA1) mRNA was measured by in situ hybridization as previously described by our laboratory (13). For details, see the Supplemental Appendix.

STATISTICAL ANALYSIS. All data are presented as mean ± SD. Goodness-of-fit tests using Kolmogorov-Smirnov and data visualization (histogram and Q-Q plots) were used to assess normal distribution of data and to look for outliers. No data points were excluded from analysis due to outlier status. Pearson correlation analyses were performed to identify linear associations between variables. Student's *t*-test was used for between group comparisons. Multilevel analysis was used to analyze within-group comparisons of chymase activity among cardiac chambers (RA, LA, and LV). All analyses were performed using SAS version 9.4 (SAS Institute, Cary, North Carolina), with a 2-sided $p < 0.05$ considered to be statistically significant.

RESULTS

CARDIAC MAGNETIC RESONANCE IMAGING. Supplemental Table 1 lists the demographic data on

FIGURE 3 TEM of LA of 3 Patients With MR

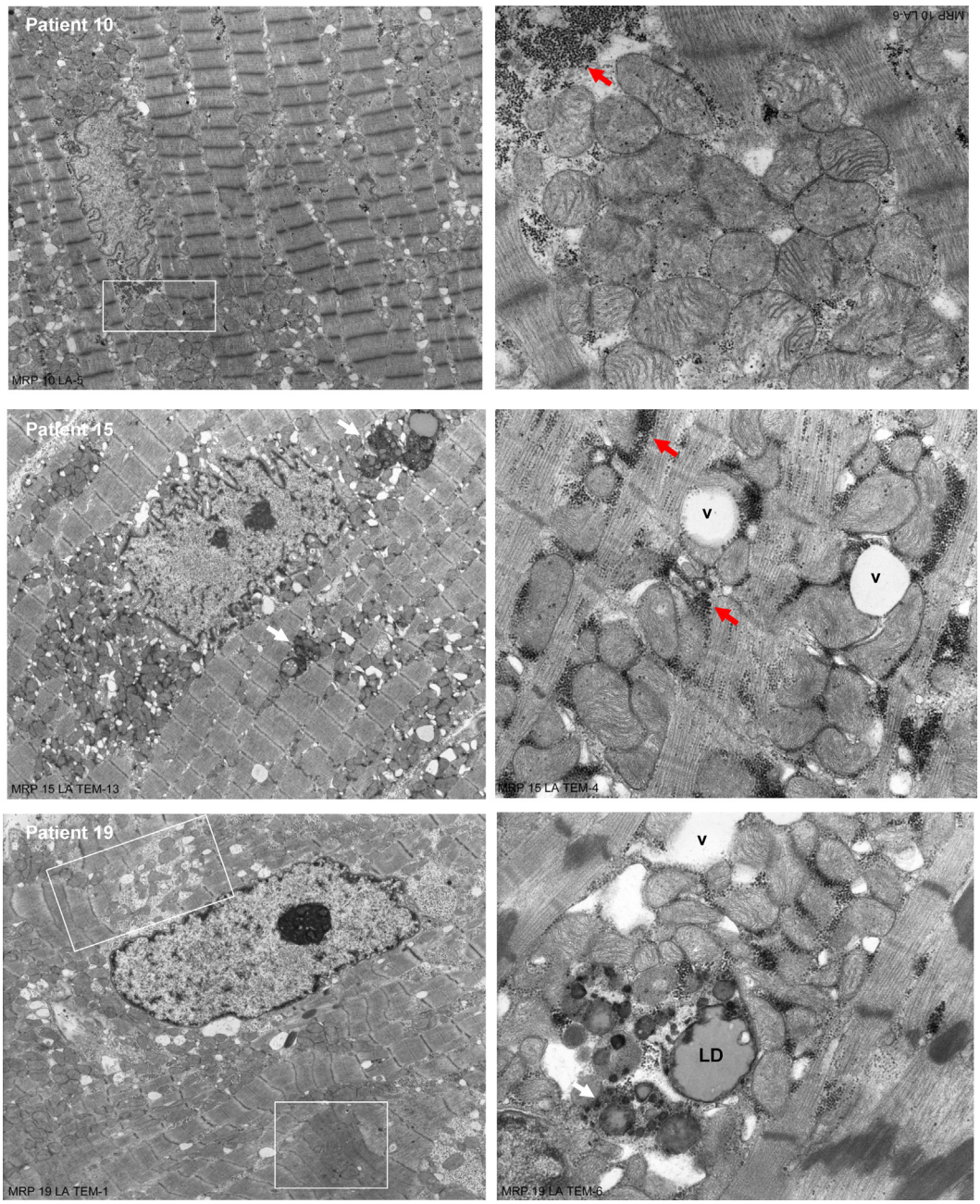

Transmission electron microscopy (TEM) of LA of 3 patients with MR demonstrates extensive myofibrillar breakdown with distortion of the z-disc and sarcomere, as well as collections of many small, disorganized, and multiple shaped mitochondria with sparsely packed cristae, extensive nonmembrane-bound vacuoles (v), lipid droplets (LD), lipofuscin **(black arrows)** and glycogen accumulation **(red arrows)**. **Patient #10** is a 50-year-old white male, with a LA maximum volume (MV) if 280 ml. His LA EF of 27% has multiple areas of myofibrillar loss that at a higher magnification **(square)** show the replacement by glycogen accumulation **(dark black dots)**, empty vacuoles, and clusters of mitochondria with either dissolved or broken cristae. **Patient #15** is a 59-year-old white male, with a LAMV of 71 ml. His LA EF of 50% also demonstrates large accumulations of glycogen and variably sized mitochondria that replace areas of myofibrillar loss. **Patient #19** is a 59-year-old black male, with a LAMV of 88 ml. His LA EF of 40% has multiple areas of sarcomere stretch and contraction **(box)** with distorted z-discs and lipid droplets (LD), and electron dense particles of lipofuscin-containing lipid droplets **(arrows)**. Abbreviations as Figure 1.

20 patients with MR, and Supplemental Table 2 lists the underlying cardiac conditions in the control subjects with nonfailing hearts. Supplemental Table 3 presents the MR regurgitant volume (median 54 ml) and regurgitant fraction (median 44%), both of which were consistent with severe MR. **Figure 1A** demonstrates a nearly 2-fold increase in MR LV end-diastolic volume; however, LV ejection fraction did not differ from the age-matched normal subjects. In contrast, LA maximum and minimum volumes were increased 2- and 3-fold, respectively, and total LA EF was decreased below that in age-matched normal subjects (**Figure 1A**, right panel). The simultaneous LA and LV time–volume curves showed that LA maximum volume surpassed LV end-systolic volume in the patients with MR. This, coupled with the decrease in LA EF, indicated a loss of pre-load reserve in MR (**Figure 1A**) that was not evident in the LV due to ejection into the low-pressure LA (**Figure 1B**). **Figure 2A** demonstrates the marked increase in global LA size and the LA appendage in a 2-chamber view. The accompanying surface 3-dimensional curvature display demonstrates the marked distortion of LA geometry with severe MR (**Figure 2B**). In addition, LV function was well preserved despite the change to a more spherical geometry of the apex, as previously described in patients with isolated MR (16). Total LA EF was negatively related to increasing LA maximum volume (**Figure 2C**), whereas LV ejection fraction had no relation to LV end-diastolic volume (**Figure 2D**). In contrast, RA and RV volumes and RVEF did not differ from age-matched normal subjects (Supplemental Figure 1).

TRANSMISSION ELECTRON MICROSCOPY MYOCARDIAL ULTRASTRUCTURE. Ten of the 20 patients who underwent cardiac magnetic resonance imaging had transmission electron microscopy (TEM) analysis. **Figure 3** demonstrates representative examples of 3 patients with total LA EF ranging from 27% to 50%. In all 10 patients, LA myocytes demonstrated similar ultrastructural changes marked by mitochondrial disarray, blurring, or thickening of the z disc, as well as extensive areas of myofibrillar breakdown. Multiple areas of sarcomere breakdown were replaced by numerous nonmembrane-bound vacuoles (**Figure 3**, right panel; Patient #15) in juxtaposition to clusters of small round mitochondria with sparse disorganized cristae (**Figure 3**, right panel; Patient #10). There was extensive disruption of a mitochondrial linear registry that should normally be in close proximity to myofibrils and straddled 1 sarcomere in all 3 patients. In addition, glycogen accumulation and lipid droplets (**Figure 3**, right panel; Patient #19) spanned the peri-nuclear, interfibrillar, and subsarcolemmal areas of the LA myocyte. In these representative patients, clusters of mitochondria and glycogen accumulation (**Figure 3**, red arrows; Patients # 10 and 15) filled areas of myofibrillar breakdown in peri-nuclear, interfibrillar, and subsarcolemmal areas.

MYOFIBRILLAR AND DESMIN BREAKDOWN IN LA AND LV CARDIOMYOCYTES. LAs of Patients #'s 7, 3, and 19 had extensive atrial myolysis demonstrated by large empty spaces that indicated myofibrillar fragmentation on hematoxylin and eosin (**Figure 4**). **Figure 4** (lower right panel) demonstrates myosin Western blot with myosin fragmentation in the LA and LV but not the RAs of Patient # 6 and 8. These hematoxylin and eosin examples further supported the global myofibrillar degeneration in LA myocytes evident in the TEM images in **Figure 3**.

CHYMASE ACTIVITY IN RA, LA AND LV. LA chymotryptic activity was 6-fold higher than RA and LV chymotryptic activity in MR hearts (**Figure 5A**). In 11 MR LA biopsies, chymotryptic activity correlated with TGF-β_1 protein levels (**Figure 5B**). LA chymotryptic activity and TGF-β_1 levels were negatively related to total LA EF (**Figures 5C and 5E**) and positively related to LA minimum volume (**Figures 5D and 5F**).

FIBROSIS IN MR LA. There was extensive LA fibrosis in patients with MR. Compared with a nonfailing LA (**Figure 6A**), MR LA immunohistochemistry demonstrated desmin breakdown and had a marked amount of chymase in the interstitium adjacent to a mast cell (**Figure 6B**), as further identified by Giemsa staining in mast cell granules (**Figure 6C**). There was extensive replacement fibrosis in the MR LA, as demonstrated in the trichome image (**Figure 6D**), and an increase in volume percent collagen quantitated with picric acid Sirius red collagen analysis (8.84 ± 3.9 vs. 4.71 ± 0.8; $p = 0.001$) (**Figure 6E**). The amount of collagen negatively correlated with the decrease in total LA EF (**Figure 6F**).

CHYMASE WITHIN LA MYOCYTES. **Figure 7** demonstrates chymotryptic-like activity within cardiomyocytes and mast cell (MC) by in situ assay analysis (deep blue color, **Figures 7A and 7C**). In the adjacent cardiomyocytes, there was evidence of chymotryptic activity identified by blue staining in the cross section (**Figure 7A**) and by blue dots, largely seen between z discs associated with the myofibrils (**Figure 7C**). The increased chymotryptic activity was prevented by pre-treatment with the specific chymase inhibitor, TEI-F0086 (**Figures 7B and 7D**), especially in the chymase-laden mast cells in **Figures 7A and 7B**,

FIGURE 4 Hematoxylin & Eosin Staining in LAs of Patients #'s #7, #3, and #19

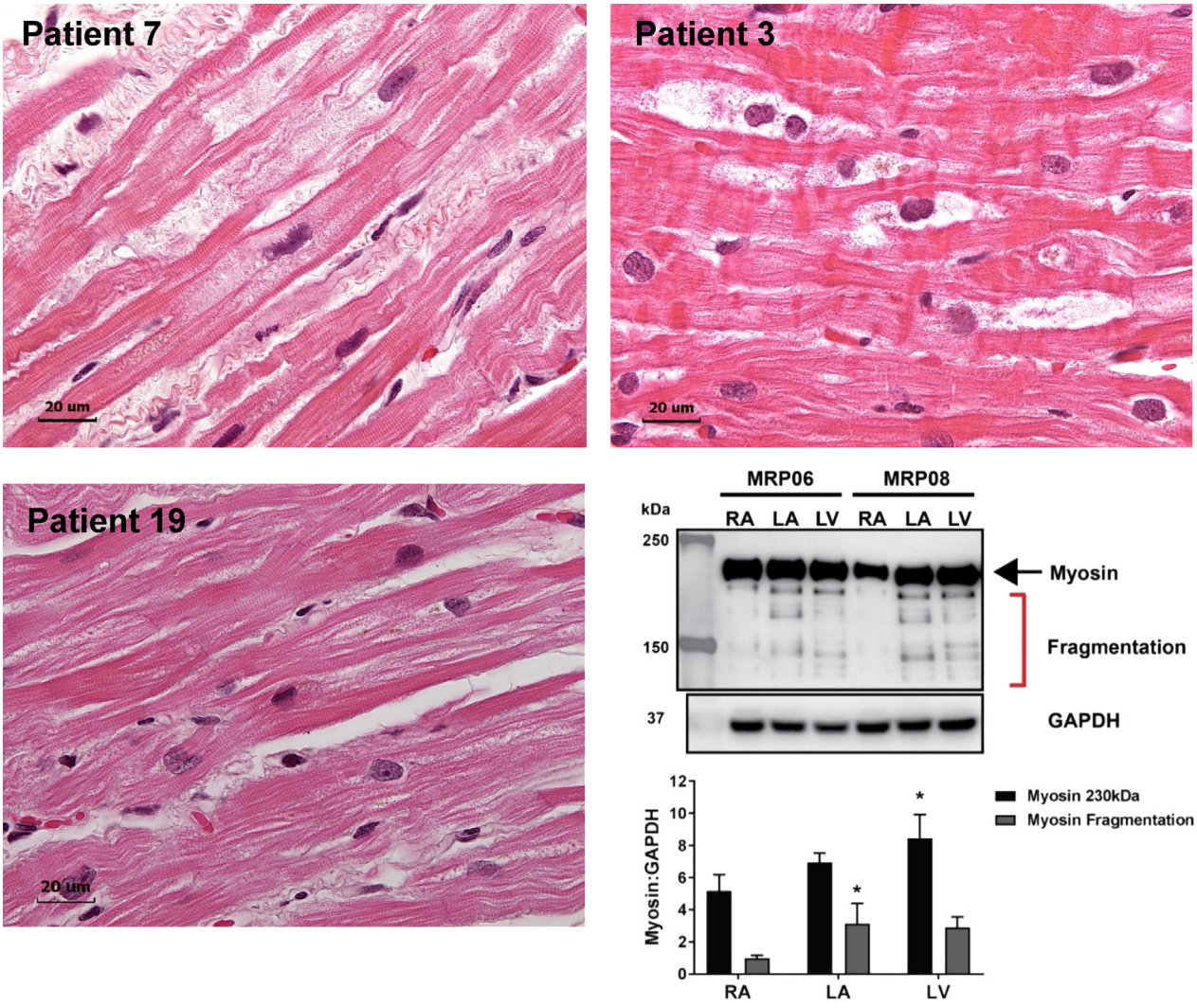

There is extensive atrial myolysis demonstrated by large empty spaces and myofibrillar fragmentation. **Patient #7** is a 52-year-old white male, with a LAMV of 112 ml and a LA EF of 25%. **Patient #3** is a 60-year-old white male, with a LAMV of 88 ml and LA EF of 50%. **Patient #19** is a 59-year-old black male, with a LAMV of 88 ml and a LA EF of 40%. **Lower right panel** demonstrates Western blot of myosin fragmentation in LA and LV but not the right atrium (RA) of Patients # 6 and 8 with MR. *$p < 0.05$ versus RA. Abbreviations as in Figures 1 and 3.

which indicated the specificity of the stain for chymase. Immunohistochemistry (Figure 7E) of MR LA demonstrated chymase (Figure 7E, red) within LA myocytes in the peri-nuclear areas (Figure 7E, arrows) and in sarcomeres in areas of desmin breakdown (Figure 7E, arrowhead). TEM immunogold images (40,000×; Figure 7F) demonstrated chymase (Figure 7F, black dots) associated with myofibrillar breakdown (Figure 7F, arrowheads) and mitochondria. In situ hybridization demonstrated that chymase mRNA was largely present in endothelial cells, and in interstitial cells that were most likely fibroblasts, and heavily concentrated in mast cells in human atria (Figure 8).

DISCUSSION

New findings in the present study demonstrated that an increase in LA volume and decrease in total LA EF were associated with severe LA myocyte ultrastructural damage with a LV ejection fraction of >60% in patients with isolated MR. The decline in total LA EF was related to increasing LA volume, LA chymase activity, and extent of LA fibrosis.

FIGURE 5 LA Chymotryptic Activity

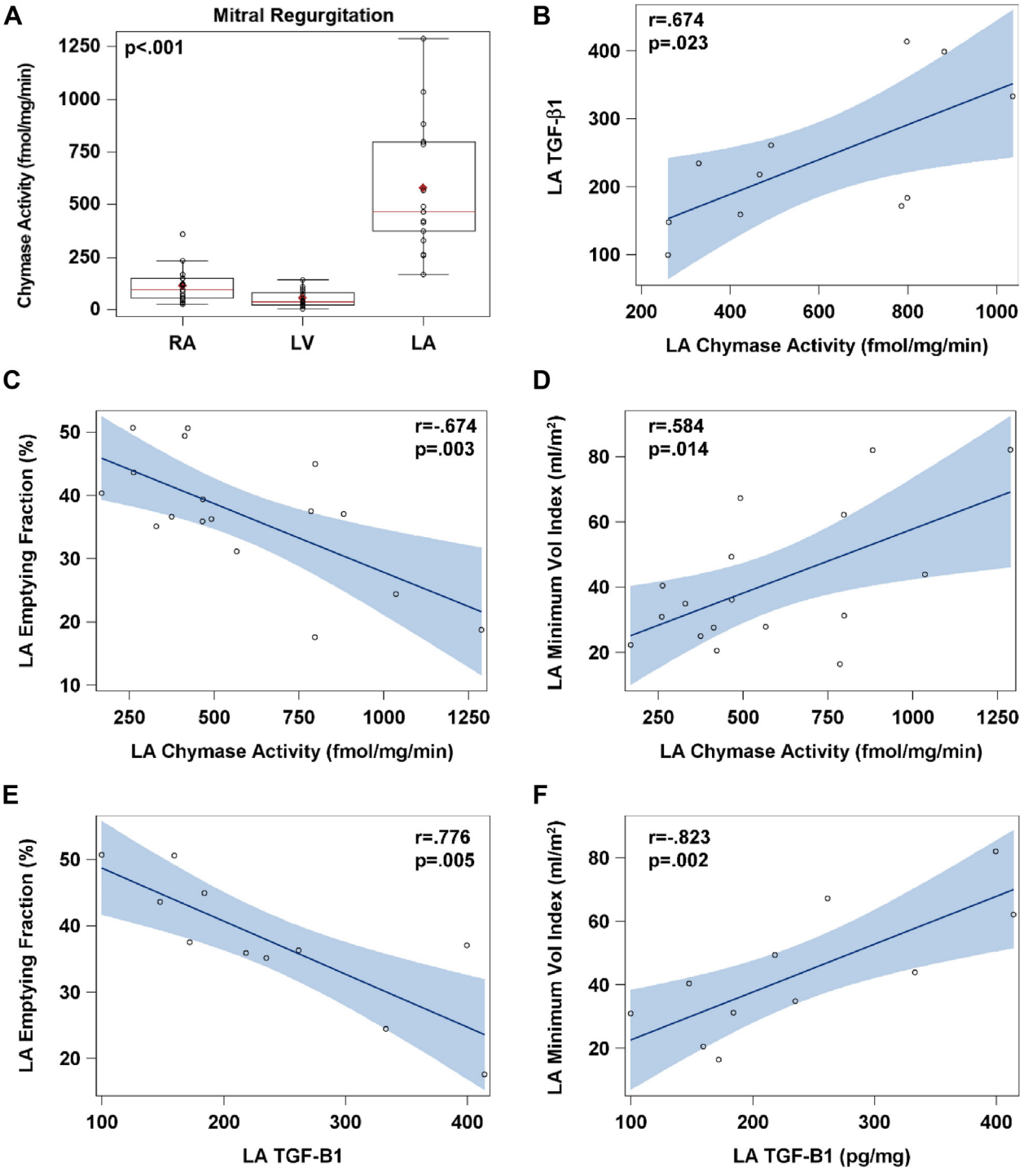

(A) LA chymotryptic activity is 6-fold higher compared with both RA and LV chymotryptic activity in MR hearts. In 11 MR LA biopsies, **(B)** chymotryptic activity correlates with transforming growth protein(TGF)-β_1 protein and **(C and D)** both total LA EF and LA minimum volume. **(E and F)** TGF-β_1 protein levels are negatively related to LA EF and positively related to LA minimum volume. Abbreviations in Figures 1 and 4.

FIGURE 6 Immunohistochemistry

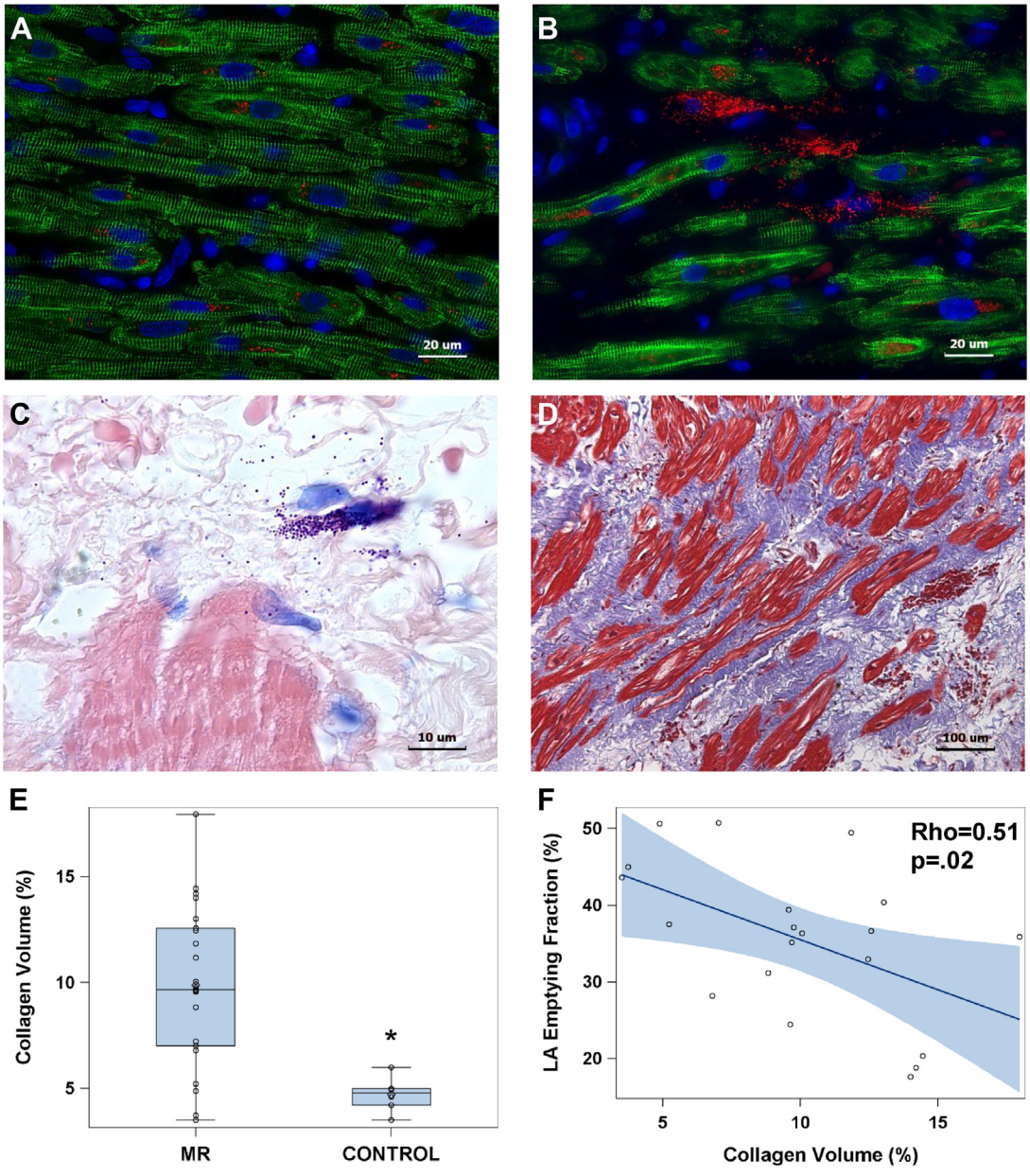

Immunohistochemistry demonstrates intact desmin **(green)** in **(A)** a nonfailing RA compared with a **(B)** MR LA where there is extensive desmin breakdown and aggregation. There is increased interstitial space in the MR LA in which there are mast cells laden with chymase **(pink)** and chymase within cardiomyocytes. **(C)** Giemsa stain shows mast cells **(dark purple)** in the interstitial space with chymase granules **(purple)** in the interstitium of extensive collagen surrounding the atrial myocardium **(red)**. **(D)** There is extensive LA fibrosis **(blue)** by trichrome stain corresponding to the empty spaces in **(B and C)** populated by chymase and mast cell granules. **(E)** There is increased LA collagen by picric acid Sirius red staining and **(F)** increased collagen relates to a decrease total LA EF. *$p < 0.001$. Abbreviations as Figures 1 and 4.

The marked fibrosis and ultrastructural damage in the LA provided further insight into our previous report of LA remodeling and dysfunction in patients with MR after MV repair (19). One-year post-surgery, despite a decrease in LA maximum and minimum volumes (20), there was a significant decrease in multiple diastolic variables below normal, including total LA EF. In the present study, a similar group of

FIGURE 7 Chymotryptic Activity Within Cardiomyocytes and Mast Cells

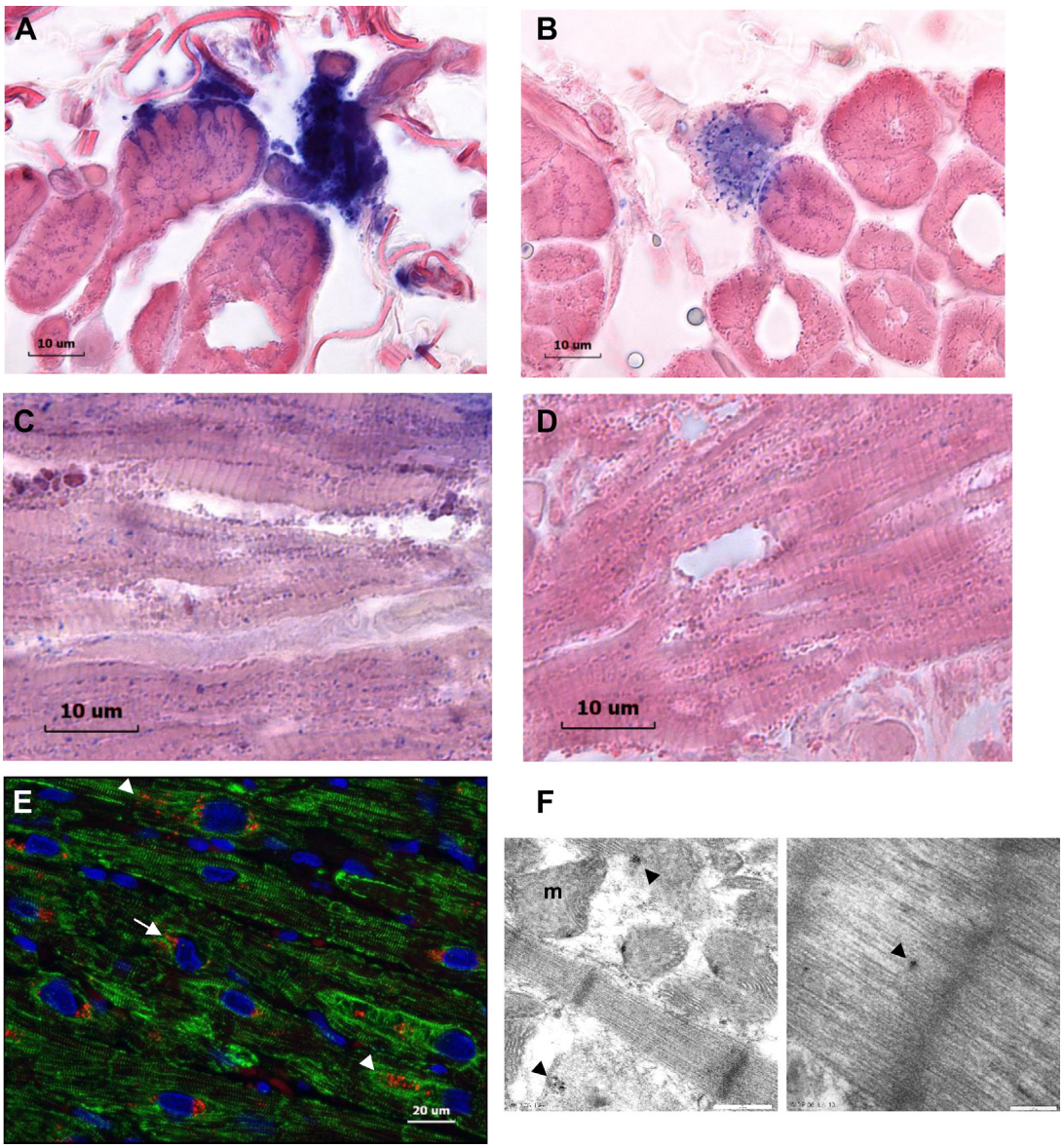

(A and C) Chymotryptic activity within cardiomyocytes and mast cells (M) **(deep blue color)** with chymotryptic activity in adjacent LA myocytes identified by **blue staining** in the **(A)** cross section and by **(C)** blue dots largely between z discs associated with the myofibrils. **(B and D)** The increased chymotryptic activity is prevented by pre-treatment with a specific chymase inhibitor, especially in the chymase-laden mast cell in (B). **(E)** Immunohistochemistry of MR LA demonstrating chymase **(red)** within LA myocyte in the peri-nuclear areas **(arrows)** and sarcomeres in areas of desmin breakdown **(arrowhead)**. **(F)** TEM immunogold image (40,000× demonstrating chymase **(black dots)** associated with myofibrillar breakdown **(arrows)** and mitochondria (m). Abbreviations as in Figures 1 and 3.

patients with LV ejection fractions >60% had extensive replacement fibrosis and LA myolysis. Total LA EF declined with a progressive increase in LA volume and fibrosis. The decrease in total LA EF with increasing LA maximum volume indicated a loss of pre-load reserve with increasing LA volume, as previously reported in a large cohort of patients who progressed from mild to moderate to severe MR (19).

LA chymase activity correlated with TGF-β protein content, and both chymase and TGF-β correlated with the increase in minimum LA volume and decline in total LA EF. The long-term effect of chymase-

FIGURE 8 In Situ Hybridization With Chymase mRNA Antisense in MR

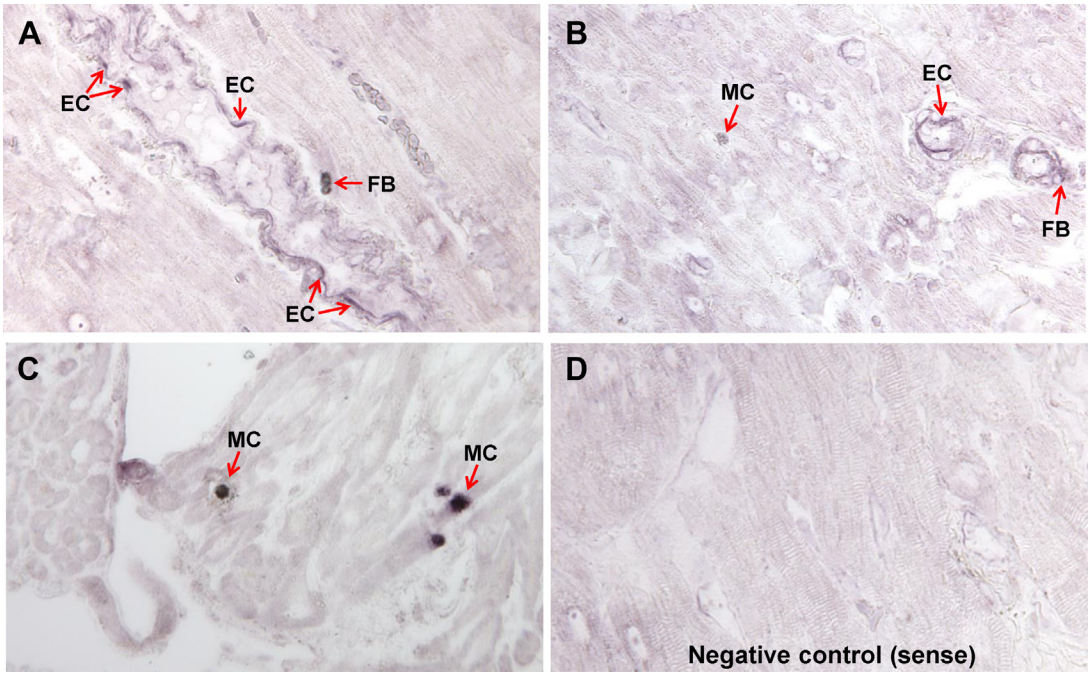

(A to C) In situ hybridization with chymase mRNA antisense in MR atria demonstrating chymase mRNA in endothelial cells (EC) lining a blood vessel and interstitial cells (most likely fibroblasts [FB]) and cells with granules consistent with mast cells (MC). There is a limited amount of chymase mRNA in myocytes. **(D)** Sense control.

mediated angiotensin II formation and activation of TGF-β could mediate the myocyte cell necrosis and the extensive replacement fibrosis noted in the MR LA. Furthermore, there was a large presence of chymase in the LA interstitium produced by mast cells and interstitial cells (most likely fibroblasts), as well as endothelial cells, which reinforced the extensive presence of chymase in the extent of LA fibrosis. In a dog model of isolated MR (21), LA interstitial fibrosis occurred within several weeks of MR induction, and paralleled increased vulnerability to atrial fibrillation. It is tempting to speculate that the greater amount of chymase activity in the thin-walled human LA, in addition to excessive stretch of MR, might make it especially prone to acute injury and subsequent fibrosis, atrial fibrillation, and a decline in the total LA EF.

Another cause for the decline in LA function was the marked amount of myofibrillar degeneration by TEM and atrial myolysis by hematoxylin and eosin and Western blot. In addition to the extracellular location of chymase, we reported chymase within cardiomyocytes of rats with volume overload of the aorto-caval fistula (13) and in dogs with ischemia–reperfusion injury (14). We showed a similar presence of chymase within LA myocytes by TEM immunogold that was functionally verified by in situ chymotryptic activity within the MR LA myocytes. Chymase uptake in adult rat cardiomyocytes causes myosin breakdown that is attenuated by a dynamin inhibitor that prevents chymase uptake (14).

Long-term treatment with an oral chymase inhibitor preserved desmin and myosin architecture and cardiomyocyte function in dogs with experimentally induced MR (22). In a subsequent analysis of these same dogs, chymase inhibition decreased LA fibrofatty infiltration, preserved myocyte architecture, and significantly increased atrial booster pump function (Supplemental Figure 2). In this pre-clinical study, dogs had only the alpha isoform of chymase that was most similar to humans, whereas rodents had both alpha and multiple beta isoforms that degraded rather than formed angiotensin II.

Taken together with the results of in situ hybridization, these data supported the contention that the presence and activity of chymase within cardiomyocytes was largely due to uptake from adjacent cells, with minimal evidence of cardiomyocyte in situ

production of chymase mRNA. Finally, the marked increase in LA chymase activity compared the activity in the RA and LV was completely unexpected. This calls for consideration of a clinically actionable finding with regard to the pathophysiology of LA fibrosis in MR, especially because a new type of chymase inhibitor, BAY1142524, is being studied in a phase II clinical trial (A Single-blind Pilot Study to Investigate Safety and Tolerability of the Chymase Inhibitor BAY1142524 in Clinically Stable Patients With Left-ventricular Dysfunction [CHIARA MIA 1]; NCT02452515) to treat patients with LV dysfunction after myocardial infarction.

Increased adrenergic drive (23–25), tumor necrosis factor–α (24), oxidative stress (in particular, xanthine oxidase) (18), and activation of Matrix metalloproteinase and calpain (6,7) have also been reported in this multifaceted myocardial response to isolated MR. β_1-receptor blockade attenuated myofibrillar loss and improved cardiomyocyte shortening and LV systolic function in the dog model of isolated MR (26,27). β_1-receptor blockade also improved LV ejection fraction and LV diastolic function during a 2-year follow-up in patients with asymptomatic moderate MR (28). It may be tempting to speculate that β_1-receptor blockade has a beneficial effect on the MR LA and LV cardiomyocyte sarcomeric and mitochondrial architecture, loss of major cytoskeletal intermediate filament desmin, and myofibrillar degeneration (1,2). Nevertheless, MR is a mechanical problem, and the timing for surgical intervention is still in question, especially in the asymptomatic patient with moderate to severe MR and LV ejection fraction of >60%.

CONCLUSIONS

In the present study, extensive LA fibrosis that was related to an increase in LA size and total LA EF supported the contention that the thin-walled LA was a harbinger of early LV myocardial damage. This was also in keeping with LA size as an independent predictor of outcome in isolated MR but added an important clinical message that the LA was not merely a bystander of MR but rather was actively involved in the pathophysiology of the disease (6,7). With the unreliability of the LV ejection fraction, future studies could consider LA size and total LA EF for timing of surgical intervention in asymptomatic moderate to severe MR.

ADDRESS FOR CORRESPONDENCE: Dr. Louis J. Dell'Italia, Birmingham VA Medical Center, 700 South 19th Street, Birmingham, Alabama 35233. E-mail: louis.dellitalia@va.gov.

PERSPECTIVES

COMPETENCY IN MEDICAL KNOWLEDGE: LA enlargement and a reduced emptying fraction are associated with chymase activation and extensive LA fibrosis with LV ejection fractions >60%.

TRANSLATIONAL OUTLOOK: Because of the unreliability of LV ejection fractions, further studies are needed to define the limits of LA enlargement and dysfunction for surgical timing for MV surgery in isolated MR.

REFERENCES

1. Miller JD, Suri RM. Left ventricular dysfunction after degenerative mitral valve repair: a question of better molecular targets or better surgical timing? J Thorac Cardiovasc Surg 2016;152:1071–4.

2. Quintana E, Suri RM, Thalji NM, et al. Left ventricular dysfunction after mitral valve repair-the fallacy of "normal" preoperative myocardial function. J Thorac Cardiovasc Surg 2014;148:2752–62.

3. Enriquez-Sarano M, Suri RM, Clavel MA, et al. Is there an outcome penalty linked to guideline-based indications for valvular surgery? Early and long-term analysis of patients with organic mitral regurgitation. J Thorac Cardiovasc Surg 2015;150:50–8.

4. Le Tourneau T, Messika-Zeitoun D, Russo A, et al. Impact of left atrial volume on clinical outcome in organic mitral regurgitation. J Am Coll Cardiol 2010;56:570–8.

5. Rusinaru D, Tribouilloy C, Grigioni F, et al. Mitral Regurgitation International DAtabase (MIDA) Investigators. Left atrial size is a potent predictor of mortality in mitral regurgitation due to flail leaflets: results from a large international multicenter study. Circ Cardiovasc Imaging 2011;4:473–81.

6. Corradi D, Callegari S, Benussi S, et al. Myocyte changes and their left atrial distribution in patients with chronic atrial fibrillation related to mitral valve disease. Hum Pathol 2005;36:1080–9.

7. Corradi D, Callegari S, Benussi S, et al. Regional left atrial interstitial remodeling in patients with chronic atrial fibrillation undergoing mitral-valve surgery. Virchows Arch 2004;445:498–505.

8. Chen HC, Chang JP, Chang TH, et al. Enhanced expression of ROCK in left atrial myocytes of mitral regurgitation: a potential mechanism of myolysis. BMC Cardiovasc Disord 2015;15:33.

9. Chang JP, Chen MC, Liu WH, et al. Atrial myocardial nox2 containing NADPH oxidase activity contribution to oxidative stress in mitral regurgitation: potential mechanism for atrial remodeling. Cardiovasc Pathol 2011;20:99–106.

10. Posina K, McLaughlin J, Rhee P, et al. Relationship of phasic left atrial volume and emptying function to left ventricular filling pressure: a cardiovascular magnetic resonance study. J Cardiovasc Magn Reson 2013;15:99.

11. Ahmad S, Simmons T, Varagic J, Moniwa N, Chappell MC, Ferrario CM. Chymase-dependent generation of angiotensin II from angiotensin-(1-12) in human atrial tissue. PLoS One 2011;6:e28501.

12. Dell'Italia LJ, Collawn JF, Ferrario CM. Multifunctional role of chymase in acute and chronic tissue injury and remodeling. Circ Res 2018;122:319–36.

13. Powell PC, Wei C-C, Fu L, et al. Chymase uptake by cardiomyocytes results in myosin degradation in cardiac volume overload. Heliyon 2019;5:e01397.

14. Zheng J, Wei CC, Hase N, et al. Chymase mediates injury and mitochondrial damage in cardiomyocytes during acute ischemia/reperfusion in the dog. PLoS One 2014;9:e94732.

15. Feng W, Nagaraj H, Gupta H, et al. A dual propagation contours technique for semi-automated assessment of systolic and diastolic cardiac function by CMR. J Cardiovasc Magn Reson 2009:13;11:30.

16. Schiros CG, Dell'Italia LJ, Gladden JD, et al. Magnetic resonance imaging with 3-dimensional analysis of left ventricular remodeling in isolated mitral regurgitation: implications beyond dimensions. Circulation 2012;125:2334–42.

17. Ahmed MI, Guichard JL, Rajasekaran NS, et al. Disruption of desmin-mitochondrial architecture in patients with regurgitant mitral valves and preserved ventricular function. J Thorac Cardiovasc Surg 2016;152:1059–70.

18. Ahmed MI, Gladden JD, Litovsky SH, et al. Increased oxidative stress and cardiomyocyte myofibrillar degeneration in patients with chronic isolated mitral regurgitation and ejection fraction >60%. J Am Coll Cardiol 2010;55:671–9.

19. Schiros CG, Ahmed MI, McGiffin DC, et al. Mitral annular kinetics, left atrial, and left ventricular diastolic function post mitral valve repair in degenerative mitral regurgitation. Front Cardiovasc Med 2015;2:31.

20. Ren B, de Groot-de Laat LE, Geleijnse ML. Left atrial function in patients with mitral valve regurgitation. Am J Physiol Heart Circ Physiol 2014;307:H1430–14307.

21. Verheule S, Wilson E, Everett T 4th, Shanbhag S, Golden C, Olgin J. Alterations in atrial electrophysiology and tissue structure in a canine model of chronic atrial dilatation due to mitral regurgitation. Circulation 2003;107:2615–22.

22. Pat B, Killingsworth C, Shi K, et al. Chymase inhibition prevents fibronectin and myofibrillar loss and improves cardiomyocyte function and LV torsion angle in dogs with isolated mitral regurgitation. Circulation 2010;122:1488–95.

23. Grossman PM, Linares OA, Supiano MA, Oral H, Mehta RH, Starling MR. Cardiac-specific norepinephrine mass transport and its relationship to left ventricular size and systolic performance. Am J Physiol Heart Circ Physiol 2004;287:H878–88.

24. Zheng J, Yancey DM, Ahmed MI, et al. Increased sarcolipin expression and adrenergic drive in humans with preserved left ventricular ejection fraction and chronic isolated mitral regurgitation. Circ Heart Fail 2014;7:194–202.

25. Oral H, Sivasubramanian N, Dyke DB, et al. Myocardial proinflammatory cytokine expression and left ventricular remodeling in patients with chronic mitral regurgitation. Circulation 2003;107:831–7.

26. Pat B, Killingsworth C, Denney T, et al. Dissociation between cardiomyocyte function and remodeling with beta-adrenergic receptor blockade in isolated canine mitral regurgitation. Am J Physiol Heart Circ Physiol 2008;295:H2321–7.

27. Tsutsui H, Spinale FG, Nagatsu M, et al. Effects of chronic beta-adrenergic blockade on the left ventricular and cardiocyte abnormalities of chronic canine mitral regurgitation. J Clin Invest 1994;93:2639–48.

28. Ahmed MI, Aban I, Lloyd SG, et al. A randomized controlled phase IIb trial of beta(1)-receptor blockade for chronic degenerative mitral regurgitation. J Am Coll Cardiol 2012;60:833–8.

KEY WORDS chymase, fibrosis, left atrium, left ventricle, mitral regurgitation, mitral valve

APPENDIX For an expanded Methods section as well as supplemental figures and tables, please see the online version of this paper.